nature biotechnology

Programmable ligand-controlled riboregulators of eukaryotic gene expression

Travis S Bayer & Christina D Smolke

Recent studies have demonstrated the importance of noncoding RNA elements in regulating gene expression networks[1,2]. We describe the design of a class of small *trans*-acting RNAs that directly regulate gene expression in a ligand-dependent manner. These allosteric riboregulators, which we call antiswitches, are made fully tunable and modular by rational design. They offer flexible control strategies by adopting active or inactive forms in response to ligand binding, depending on their design. They can be tailor-made to regulate the expression of target transcripts in response to different cellular effectors. Coupled with *in vitro* selection technologies for generating nucleic acid ligand-binding species[3,4], antiswitches present a platform for programming cellular behavior and genetic networks with respect to cellular state and environmental stimuli.

In recent years, *cis* and *trans* RNA elements have become well recognized as important regulators of gene expression. Cells use diverse noncoding RNA elements to regulate complex genetic networks such as those involved in developmental timing and circadian clocks[1,2]. These include antisense RNAs[5–7], small *trans*-acting RNAs (taRNAs) that bind target mRNA; microRNAs[8] (miRNAs), which interact with complementary sequences in mRNA and the genome; small interfering RNAs[9] (siRNAs), which function through the RNA interference (RNAi) pathway in metazoans; ribozymes[10], or catalytic RNA molecules; and riboswitches[11–13], *cis*-acting metabolite-binding structures in mRNAs that modulate translation initiation, disrupt transcriptional termination or cleave mRNA by ribozyme mechanisms. Recent studies have demonstrated the prevalence of these RNA-based regulators across diverse organisms from prokaryotes to humans[14–16].

Aptamers are nucleic acid species that bind specific ligands and are generated through *in vitro* selection or SELEX (Systematic Evolution of Ligands by EXponential enrichment)[3,4]. They have been selected to bind diverse targets such as dyes, proteins, peptides, aromatic small molecules, antibiotics and other biomolecules[17]. High-throughput methods generate aptamers in a rapid and parallel manner[18]. Aptamers can impart allosteric control properties to other functional RNA molecules, allowing the construction of *in vitro* signaling aptamers, *in vitro* sensors and *in vitro* allosterically controlled ribozymes[19–21].

In addition to the widespread occurrence of RNA regulator elements in natural systems, several riboregulator systems have recently been engineered. These include, in *Escherichia coli*, *cis*-acting RNA elements that regulate relative expression levels from a two-gene transcript by controlling RNA processing and decay[22], and a combined *cis*/*trans* system in which *cis*-acting RNA elements inhibit translation and *trans*-activating RNAs bind to the *cis*-acting elements to allow translation[23]. *Cis*-acting elements that control gene expression in mammalian cells and mice through RNA cleavage, and whose activity can be regulated by a small-molecule drug and antisense oligonucleotides, have also been reported[24]. Finally, an allosteric aptamer construct was engineered that upon binding the dye tetramethylrosamine, interacts with protein transcriptional activators to induce transcription[25].

Although riboregulators provide tools for flexible genetic regulation, there is a need to couple RNA-based regulators that directly target transcripts with allosteric control. We have engineered ligand-responsive riboregulators in *Saccharomyces cerevisiae*. In principle, these modular, tunable riboregulators, which we call antiswitches, can be designed to regulate the expression of any target transcript in response to any ligand. The riboregulators use an antisense domain to control gene expression[6,26,27] and an aptamer domain to recognize specific effector ligands (**Fig. 1a**). Ligand binding at the aptamer domain induces a conformational change that allows the antisense domain to interact with a target mRNA to affect translation. In the absence of ligand, the antisense domain is sequestered in an 'antisense stem'. Similar mechanisms have been described in the construction of signaling aptamers and other allosterically controlled RNAs[28].

Specifically, we constructed an initial antiswitch, s1, using a previously selected aptamer that binds the xanthine derivative theophylline with high affinity (K_d = 0.29 μM) and specificity[29]. The antisense RNA domain is designed to base pair with a 15-nucleotide region around the start codon of a target mRNA encoding green fluorescent protein (GFP). The stem of the theophylline aptamer is redesigned so that in the absence of ligand, the antisense portion base pairs in a double-stranded region of the RNA referred to as the 'antisense stem'; upon ligand binding, another overlapping stem, the 'aptamer stem,' forms, forcing the antisense portion into a single-stranded state (**Fig. 1a**,**b**). The aptamer stem and antisense stem are designed such that the antisense stem is slightly more stable than the aptamer stem. Previous work has demonstrated that the sequence of

Division of Chemistry and Chemical Engineering, 1200 East California Blvd., MC 210-41, California Institute of Technology, Pasadena, California 91125, USA. Correspondence should be addressed to C.D.S. (smolke@cheme.caltech.edu).

Published online 20 February 2005; doi:10.1038/nbt1069

the lower theophylline aptamer stem is not critical for ligand binding[30]; we altered this sequence to interact with the antisense stem upon ligand binding.

We anticipated that in the absence of ligand and presence of target transcript, the stem sequestering the antisense is more likely to form; whereas in the presence of both ligand and target transcript, the free energy associated with the binding of theophylline (~8.9 kcal/mol[31]) and RNA stabilization in the aptamer structure would enable the aptamer stem to form, freeing the antisense domain to bind its target transcript. RNAstructure[32] was used to predict the stability of the RNA secondary structures formed. Because of the dual-stem design of the antiswitch, we anticipated that aptamer binding to its ligand and antisense binding to its target mRNA would both contribute to the structural switching of the antiswitch molecule.

The expression of antiswitches in *S. cerevisiae* was accomplished using a noncoding RNA expression construct similar to a previously described system[33] (see **Supplementary Fig. 1** online). Briefly, the RNA to be expressed was cloned between two hammerhead ribozymes known to self-cleave *in vivo*[34]. This dual hammerhead construct can be placed under the control of Pol II promoters, and when transcribed, the flanking hammerhead ribozymes cleave out from the desired RNA at an efficiency greater than 99% (see **Supplementary Table 1** online). The construct enables creation of noncoding RNAs with defined 5′ and 3′ ends that are free of potentially interfering flanking sequences. Antiswitch s1 was expressed in this construct under control of a galactose-inducible (GAL1) promoter in yeast cells. A plasmid containing a yeast enhanced GFP (yEGFP)[35] under the control of a GAL1 promoter was used to transform the same cells (**Fig. 1a**).

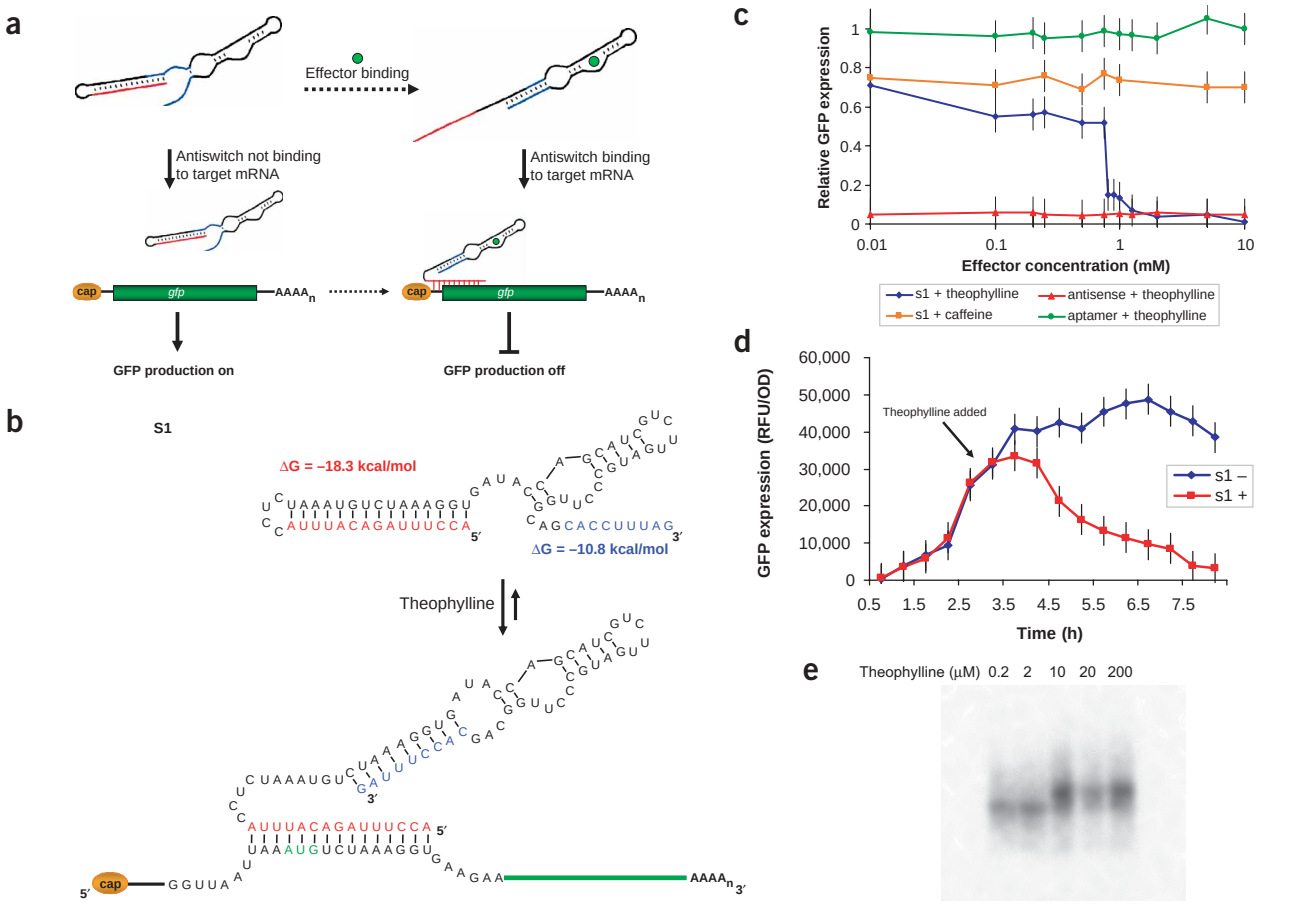

Figure 1 Design and functional activity of an antiswitch regulator. (**a**) General illustration of the mechanism by which an antiswitch molecule acts to regulate gene expression *in vivo*. The antisense sequence is indicated in red; switching 'aptamer stem' is shown in blue. In the absence of effector, the antisense domain is bound in a double-stranded region of the RNA referred to as the 'antisense stem' and the antiswitch is in the 'off' state. In this state the antiswitch is unable to bind to its target transcript, which has a *gfp* coding region, and as a result, GFP production is on. In the presence of effector, the antiswitch binds the molecule, forcing the aptamer stem to form, switching its confirmation to the 'on' state. In this state the antisense domain of the antiswitch will bind to its target transcript and through an antisense mechanism turn the production of GFP off. (**b**) Sequence and predicted structural switching of a theophylline-responsive antiswitch, s1, and its target mRNA. On s1, the antisense sequence is indicated in red; switching aptamer stem sequence is indicated in blue, the stability of each switching stem is indicated. On the target mRNA, the start codon is indicated in green. (**c**) *In vivo* GFP regulation activity of s1 and controls across different effector concentrations: aptamer construct (negative control) in the presence of theophylline (green); antisense construct (positive control) in the presence of theophylline (red); s1 in the presence of caffeine (negative control, orange); s1 in the presence of theophylline (blue). Data are presented as relative, normalized GFP expression in cells harboring these constructs against expression levels from induced and uninduced cells harboring only the GFP expression construct. (**d**) *In vivo* temporal response of s1 inhibiting GFP expression upon addition of effector to cells that have accumulated steady-state levels of GFP and antiswitch s1. No theophylline, blue; 2 mM theophylline, red. (**e**) *In vitro* affinity assays of s1 to target and effector molecules. The mobility of radiolabeled s1 was monitored in the presence of equimolar concentrations of target transcript and varying concentrations of theophylline as indicated.

Results from protein expression assays demonstrate ligand-specific, *in vivo* activity of s1 (**Fig. 1c**). Expression of antiswitch s1 in the absence of theophylline decreased GFP expression from control levels by ~30%, whereas addition of >0.8 mM theophylline decreased expression to background levels. The antisense and aptamer domains were expressed separately as controls and had the expected effects on GFP expression levels. It is interesting to note the rapid change in expression levels between 0.75 mM and 0.8 mM theophylline. The antiswitch s1 displays binary, on/off behavior rather than linearly modulating expression over a range of theophylline concentrations. This response supports the anticipated cooperative mechanism of structural switching dependent on both ligand and target mRNA.

The aptamer used in this antiswitch does not bind caffeine[29], which differs from theophylline by a single methyl group. The addition of caffeine did not change expression levels from those of an inactive switch, demonstrating that specific ligand-aptamer interactions are necessary to activate the antiswitch.

Quantitative real-time PCR (qRT-PCR) was performed on antiswitch s1 and target mRNA extracted from cells grown under different conditions to determine relative RNA levels (see **Supplementary Table 1** online). Relative levels of target transcript did not change substantially between cells harboring s1 grown in the absence or presence of high levels of theophylline, indicating that antiswitches function through translational inhibition rather than by affecting target RNA levels. In addition, the steady-state relative level of s1 was ~1,000-fold greater than target levels, although both antiswitch and target were expressed from the same promoter. This indicates that antiswitch molecules may have higher intracellular stabilities than those of mRNA, perhaps owing to stabilizing secondary structures, or are synthesized more efficiently.

The temporal response of antiswitch regulation was determined by inducing antiswitch activation through the addition of theophylline to cells expressing steady-state levels of GFP and with s1 in the 'off' state (**Fig. 1d**). GFP levels began decreasing shortly after the addition of theophylline at a rate corresponding to a half-life of ~0.5–1 h, which is consistent with the half-life of the GFP variant used in these experiments[35]. These data show that antiswitch molecules act rapidly to inhibit translation from their target mRNAs in the presence of

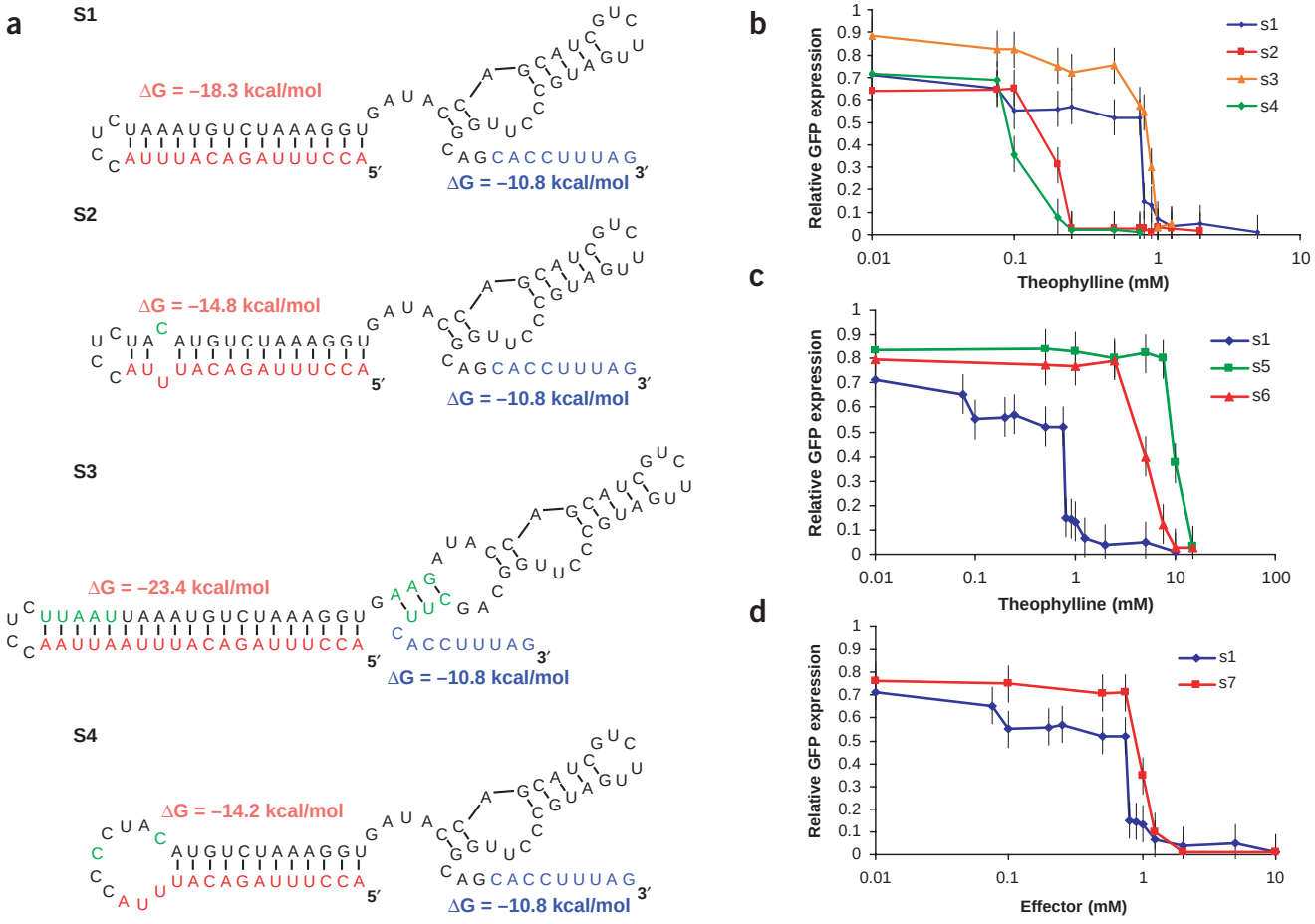

Figure 2 Tuning and expanding the switch response of an antiswitch regulator. (**a**) Predicted structures of tuned antiswitches (s2–s4), based on s1, in the absence of theophylline binding. Antisense sequences, red; switching aptamer stem sequences, blue; modified sequences, green. The stability of each switching stem is indicated. (**b**) *In vivo* GFP regulation activity of s1–s4 across different theophylline concentrations: s1, initial antiswitch construct (blue); s2, destabilized antiswitch construct (red); s3, stabilized antiswitch construct (orange); s4, destabilized antiswitch construct (green). (**c**) *In vivo* GFP regulation activity of modified aptamer-antiswitch constructs (s5–s6) across different theophylline concentrations: s1, initial antiswitch construct (blue); s5, antiswitch construct with an aptamer domain having tenfold lower affinity to theophylline than that used in s1 (green); s6, destabilized modified aptamer-antiswitch construct, based on s5 (red). (**d**) *In vivo* GFP regulation activity of antiswitch constructs responsive to different small molecule effectors (s1, s7) across different effector concentrations: s1, initial antiswitch construct responsive to theophylline (blue); s7, antiswitch construct modified with a tetracycline aptamer domain, based on s1, responsive to tetracycline (red).

activating levels of effector and that the time required for target protein levels to decrease is determined by the protein's half-life.

In vitro characterization studies were conducted to examine antiswitch-ligand affinity and conformational changes associated with antiswitch response. Gel-shift experiments were conducted in the presence of equimolar amounts of a short target transcript (200 nucleotides), containing regions upstream and downstream of the start codon, labeled s1, and varying concentrations of theophylline to examine antiswitch ligand affinity (**Fig. 1e**). A sharp shift in antiswitch mobility between 2 and 10 μM theophylline was presumably due to binding of both theophylline and target. Nuclease mapping in the presence of ligand alone was also conducted to investigate antiswitch conformational changes (see **Supplementary Fig. 2** online). These data show that antiswitch molecules need much higher concentrations of ligand alone (200 μM–2 mM) than of ligand with target (2–10 μM) to exhibit conformational changes, supporting the idea of cooperative effects of ligand and target on antiswitch conformational dynamics.

The *in vivo* data report the concentration of effector molecules in the medium, and we expected that the intracellular concentration of these molecules would be much lower owing to transport limitations across the membrane. One study reported over a 1,000-fold drop in theophylline concentration across the *E. coli* membrane[36]. The *in vitro* experiments indicate that ligand binding and structural switching occurred over narrow concentration ranges, much lower than the extracellular concentrations reported in the *in vivo* studies. These data indicate that in the presence of target, *in vitro* antiswitch conformational changes display a sharp binary response to ligand concentrations in the low micromolar range, which is probably indicative of the intracellular concentrations of theophylline in these studies.

The switching behavior of the antiswitch platform is dependent on the conformational dynamics of the RNA structures; therefore it should be possible to tune switching behavior in a straightforward manner by altering the thermodynamic properties of the antiswitch, particularly the absolute and relative stabilities of the antisense stem and the aptamer stem. To explore the dynamic range of switch behavior, we created several antiswitches (s2–s4) with varying antisense and aptamer stem stabilities (**Fig. 2a**). We anticipated that these altered antiswitches would expand the concentration range over which the change in gene expression was observed and increase the dynamic range of GFP expression.

Increasing antisense stem stability by the addition of base pairs created switches that required higher concentrations of theophylline to affect gene expression, whereas decreasing stem stability created switches that inhibited GFP expression at lower theophylline concentrations. For example, antiswitch s2 differs from antiswitch s1 by a single nucleotide (A21 to C) (**Fig. 2a**). This mutation introduces a mismatched pair in the antisense stem so that in the absence of ligand the construct is less thermodynamically stable. As a result, s2 exhibited altered switching dynamics; theophylline concentrations >0.2 mM inhibited gene expression, compared to 0.8 mM for construct s1 (**Fig. 2b**). Alternately, increasing the stability of the antisense stem creates a switch that requires higher concentrations of theophylline to inhibit expression.

Antiswitch s3 was designed with an antisense stem five nucleotides longer than that of s1 and an aptamer stem with 3 bp of the lower stem formed, increasing the absolute stem stabilities. As a result of this increased stability, s3 switched from GFP expression to inhibition of GFP at $\sim$1.25 mM theophylline (**Fig. 2b**), roughly 1.5-fold greater than the concentration required to switch s1, and sixfold greater than that required to switch s2. Furthermore, s3, in the 'off' state, resulted in higher levels of GFP expression, 10% versus 30% inhibition from full expression levels in induced cells harboring only the GFP construct. Antiswitch s4 was constructed to examine the effects of further destabilizing the antisense stem. This antiswitch includes an altered loop sequence (U18 to C) which further destabilizes the antisense stem from s2. Assays indicated that s4 further expanded the dynamic switching behavior of the antiswitch construct, exhibiting switching at 0.1 mM theophylline (**Fig. 2b**).

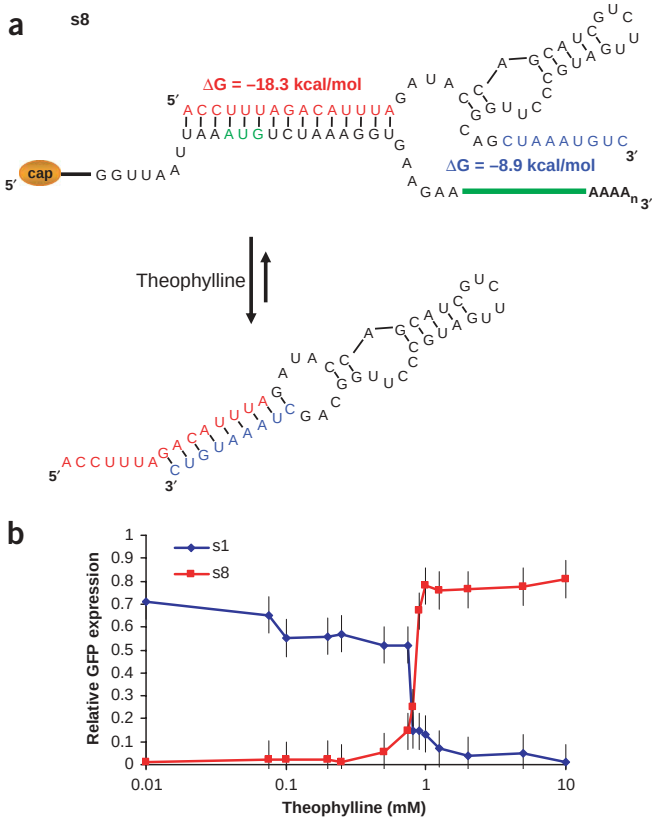

Figure 3 Redesign and characterization of an 'on' antiswitch regulator. (**a**) Sequence and structural switching of an 'on' antiswitch regulator (s8) responsive to theophylline. The antisense sequence is indicated in red; switching aptamer stem sequence is indicated in blue; the stability of each switching stem is indicated. On the target mRNA, the start codon is indicated in green. s8 is designed such that in the absence of theophylline the antiswitch is 'on' or the antisense domain is free to bind to its target. In the presence of theophylline, the antiswitch undergoes a conformational change to the 'off' state such that the antisense domain is bound in a double-stranded RNA stem that is part of the aptamer stem. (**b**) *In vivo* GFP regulation activity of 'on' and 'off' antiswitch constructs across different theophylline concentrations: s1, initial 'off' antiswitch construct (blue); s8, redesigned 'on' antiswitch construct, based on s1 (red).

To demonstrate the modularity of the antiswitch design platform, we constructed and characterized several different antiswitch molecules by swapping different aptamer domains (see **Supplementary Fig. 3** online). The antisense stem and the switching aptamer stem were kept identical to previous designs because the target transcript was kept the same, while the aptamer domains were changed. To further explore the range of ligand responsiveness in designed antiswitches, we constructed a switch s5 using a previously characterized aptamer exhibiting lower affinity to theophylline[29]. This aptamer has a K_d approximately tenfold higher than the aptamer used in s1–s4. In addition, the response of this antiswitch was tuned by destabilizing

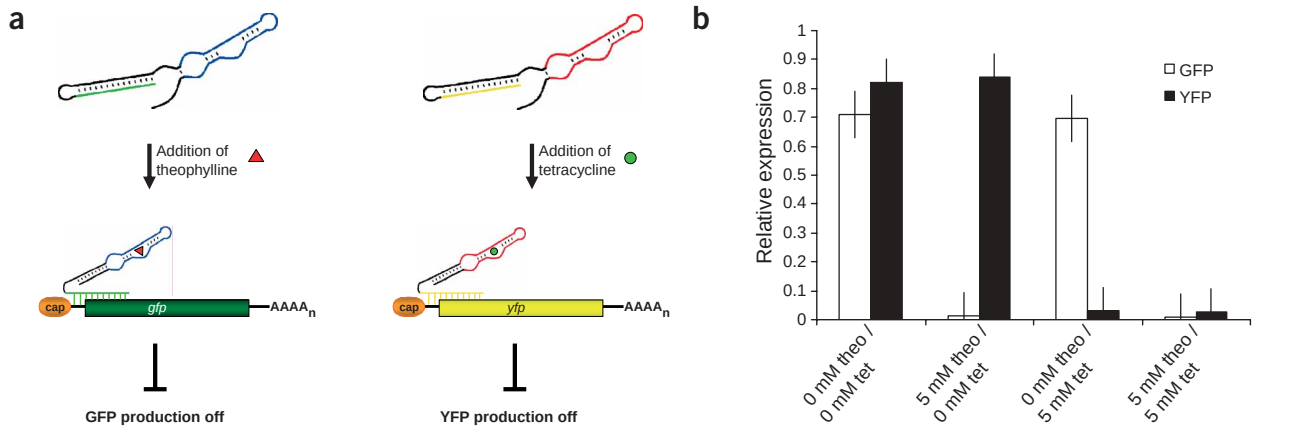

Figure 4 Simultaneous regulation of multiple genes through multiple antiswitch regulators. (**a**) Illustration of the mechanism by which two independent antiswitch molecules act to regulate the expression of multiple target genes *in vivo*. In the absence of their respective effectors, the antiswitches are in the 'off' state and are unable to bind to their target transcripts. In this state, both GFP and YFP production is on. In the presence of theophylline, one antiswitch switches its conformation to the 'on' state and turns off GFP production. In the presence of tetracycline, the second antiswitch switches its conformation to the 'on' state and turns off YFP production. These antiswitches act independently of each other to provide combinatorial control over genetic circuits. (**b**) *In vivo* regulation activity of two antiswitch constructs (s1, s9) against their respective targets (GFP, YFP) in the presence or absence of their respective effector molecules (theo, theophylline; tet, tetracycline). Relative YFP expression (black); relative GFP expression (white).

the antisense stem in a manner identical to s2, creating s6. To further test the modularity of this platform, we constructed an antiswitch with a previously characterized aptamer to tetracycline[37]. This aptamer has an affinity to tetracycline similar to that of the theophylline aptamer used in s1–4 (K_d = 1 μM).

The data in **Figure 2** support the modularity of the antiswitch platform to different aptamer domains. The modified theophylline aptamers exhibited an altered response to ligand concentrations from s1–4. As expected, the switching for s5 and s6 occurred at higher theophylline concentrations (**Fig. 2c**). s5, which contains an aptamer domain with a tenfold higher K_d than the aptamer domain in s1, switched at approximately a tenfold higher theophylline concentration. In addition, the tetracycline antiswitch s7 showed similar switch dynamics as s1–4, suggesting that the response curve observed is a general feature of designed antiswitches (**Fig. 2d**).

We examined flexibility by redesigning the antiswitch platform to construct an 'on' antiswitch from the aptamer and antisense domains used in the design of s1. We constructed antiswitch s8, which inhibits expression in the absence of theophylline, but allows expression in the presence of theophylline, using similar design principles. This switch displayed its antisense domain in the absence of ligand, leaving it free to interact with the target mRNA, while sequestering the antisense in the aptamer stem when ligand was present (**Fig. 3a**). s8 displayed dynamic behavior similar to that of s1 (switching around 1 mM theophylline), as was expected owing to similar base pairing energetics (**Fig. 3b**). This functional 'on' switch demonstrates the flexibility of the antiswitch platform and the generality of the design themes.

The modular nature of the antiswitch platform allows for systems exhibiting combinatorial control over gene expression. To illustrate this, we introduced into cells two switches, each responsive to a different effector molecule and each regulating the protein expression of a different mRNA target: s1, a theophylline-responsive GFP regulator, and s9 (see **Supplementary Fig. 4** online), a tetracycline-responsive yellow fluorescent variant protein (Venus)[38] regulator (**Fig. 4a**). Changes in the targeting capabilities of these molecules were made by modifying the antisense stem and the switching aptamer stem while keeping the remainder of the aptamer module the same. Concurrent expression of these two antiswitches with a plasmid carrying both GFP and Venus allowed for an assay of the simultaneous regulation of gene expression by modular antiswitch design. Addition of theophylline decreased expression of GFP whereas Venus expression remained unaffected; and addition of tetracycline decreased Venus while not affecting GFP (**Fig. 4b**). Furthermore, the addition of both ligands decreased expression of both GFP and Venus. This simple system illustrates the potential of building more complex genetic circuits that are precisely regulated by multiple antiswitch constructs.

This work demonstrates that engineered, ligand-controlled, antisense RNAs, or antiswitches, are allosteric regulators of gene expression. The general design of an antiswitch is based on the conformational dynamics of RNA folding to create a dual stem molecule comprised of an antisense stem and an aptamer stem. These stems are designed such that in the absence of ligand, the free energy of the antisense stem is lower than that of the aptamer stem. Ligand and target act cooperatively to alter the conformational dynamics of these molecules and stabilize the formation of the aptamer stem and the binding of the antisense domain to its target transcript. The antiswitch platform is flexible, enabling both positive and negative regulation. The 'on' switch is designed such that in the absence or at low levels of ligand the antisense domain is free to bind to the target; however, ligand binding changes the conformational dynamics of these molecules so that the antisense domain is bound in the aptamer stem.

The switching dynamics of antiswitch regulators are amenable to tuning by forward engineering design strategies based on thermodynamic properties of RNA. Altering the free energy of the antisense domain alters the conformational dynamics of these molecules in a predictable fashion. Specifically, decreasing the stability of the antisense stem decreases the ligand concentration necessary to switch the antiswitch conformation and increasing the stability of the antisense stem increases the ligand concentration necessary to switch the conformation as well as shifts the dynamics to favor the 'off' state at low ligand levels.

In addition, the antiswitch platform is fully modular, enabling ligand response and transcript targeting to be engineered by swapping

domains within the antiswitch molecule. The ligand detection capability of antiswitches is designed separately from the targeting capability by swapping only the aptamer domain. Likewise, the targeting capability of these molecules can be designed separately from the ligand detection capability by changing both the antisense stem and the switching aptamer stem to recognize a different target sequence, while not affecting the aptamer domain.

Antiswitch molecules can potentially function across a diverse range of organisms, from prokaryotes to humans, making them useful in many different applications. One example is gene therapy, in which one would like to target specific transcripts in response to specific cellular environments that are indicative of a diseased state[39]. Antiswitches may also improve current antisense therapies by introducing cell-specific action to an already highly targeted therapy. Antiswitch technology could be used to engineer novel regulatory pathways and control loops for applications in metabolic engineering[40] and synthetic circuit design[41] by enabling the cell to sense and respond to intracellular metabolite levels and environmental signals. Antiswitches may also be useful for programmable, concentration-specific detection of intracellular molecules. Finally, they may offer an approach for creating cellular sensors and 'smart' regulators to target any gene in response to any ligand, opening new avenues for cellular control and engineering.

METHODS

Plasmid construction, cell strains, reagents. Standard molecular biology techniques were used to construct all plasmids[42]. Four different plasmid constructs were generated by cloning into the pRS314-Gal and pRS316-Gal shuttle plasmids[43]. Genes and antiswitch constructs were cloned into multicloning sites, downstream of a GAL1 promoter. These plasmids (see **Supplementary Table 2** and **Supplementary Fig. 5** online) contain an *E. coli* origin of replication (f1) and selection marker for ampicillin resistance. They also have an *S. cerevisiae* origin of replication (CEN6-ARSH4) and selection markers for tryptophan (TRP1-pRS314) and uracil (URA3-pRS316) biosynthetic genes in order to select cells harboring these plasmids in synthetic complete medium supplemented with the appropriate amino acid dropout solution[42]. In the first plasmid system, pTARGET1, yEGFP was cloned into the multi-cloning site and is located between a GAL1 promoter and ADH1 terminator. In the second plasmid system, pSWITCH1, various antiswitches were cloned between two hammerhead ribozymes, which are located between a GAL1 promoter and ADH1 terminator. In the third plasmid system, pTARGET2, a P_{GAL}-Venus-$ADH1_{term}$ construct was cloned downstream of the P_{GAL}-yEGFP-$ADH1_{term}$ construct in pTARGET1. Therefore, pTARGET2 produces two target transcripts when induced with galactose. In the fourth system, pSWITCH2, a P_{GAL}-antiswitch-$ADH1_{term}$ construct was cloned downstream of the P_{GAL}-antiswitch-$ADH1_{term}$ construct in pSWITCH1. Therefore, pSWITCH2 produces two antiswitch constructs when induced by the presence of galactose. Two sets of plasmids, pTARGET1 and pSWITCH1 or pTARGET2 and pSWITCH2, were transformed into *S. cerevisiae* simultaneously and maintained with the appropriate nutrient selection pressure. In these two plasmid sets, expression of antiswitch constructs and their targets was induced upon the addition of galactose to the medium. Oligonucleotide primers were purchased from Integrated DNA Technologies. All genes and antiswitches were PCR amplified in a Dyad PCR machine (MJ Research) with Taq DNA polymerase (Roche). The *yegfp* gene was obtained from pSVA15[35] and the *venus* gene was obtained from pCS2/Venus[38]. All antiswitch sequences were obtained using custom oligonucleotide design (see **Supplementary Table 2** online).

All plasmids were constructed using restriction endonucleases and T4 DNA ligase from New England Biolabs. Plasmids were screened by transforming into an electrocompetent *E. coli* strain, DH10B (Invitrogen; F^- *mcr*A Δ(*mrr-hsd*RMS-*mcr*BC) ϕ80d*lacZ*ΔM15 Δ*lac*X74 *deo*R *rec*A1 *end*A1 *ara*D139 Δ(*ara, leu*)7697 *gal*U *gal*K λ^- *rps*L *nup*G), using a Gene Pulser Xcell System (BioRAD) according to manufacturer's instructions. Subcloning was confirmed by restriction analysis. Confirmed plasmids were then transformed into the wild-type W303α *S. cerevisiae* strain (*MATα his3-11,15 trp1-1 leu2-3 ura3-1 ade2-1*) using standard lithium acetate procedures[44]. *E. coli* cells were grown on Luria Bertani medium (DIFCO) with 100 μg/ml ampicillin (EMD Chemicals) for plasmid selection and *S. cerevisiae* cells were grown in synthetic complete medium (DIFCO) supplemented with the appropriate dropout solution (Calbiochem). Plasmid isolation was done using Perfectprep Plasmid Isolation Kits (Eppendorf).

Protein expression assays. Yeast cells were inoculated into synthetic complete medium supplemented with the appropriate dropout solution and sugar source (2% raffinose, 1% sucrose) and grown overnight at 30 °C. Cells were back diluted into fresh medium to an OD_{600} of 0.1 and grown at 30 °C. For assaying antiswitch activity, this fresh medium contained appropriate concentrations of theophylline, caffeine, tetracycline (all from Sigma) or water (negative control) and expression was induced to a final concentration of 2% galactose, or an equivalent volume of water was added (noninduced control). After growing for 3 h, the GFP and Venus levels were assayed on a Safire (Tecan) fluorescent plate reader set to the appropriate excitation (GFP, 485 nm; Venus, 515 nm) and emission (GFP, 515 nm; Venus, 508 nm) wavelengths. For assaying the antiswitch temporal response, cells were back diluted into fresh medium containing 2% galactose. After growing in inducing medium for 3 h, theophylline or water was added and fluorescence was monitored over time. Fluorescence was normalized for cell number by dividing relative fluorescence units (RFUs) by the OD_{600} of the culture.

RNA quantification. Yeast cells were grown according to methods detailed in protein expression assays. Total RNA was extracted using standard acid phenol extraction procedures[45]. Briefly, cells were pelleted and frozen in liquid nitrogen. Pellets were resuspended in a 50 mM NaOAc (pH 5.2) and 10 mM EDTA buffer. Cells were lysed by the addition of SDS to a final concentration of 1.6% and an equal volume of acid phenol. Solutions were kept at 65 °C with intermittent vortexing for 10 min. After cooling on ice, the aqueous phase was extracted and further extraction was carried out with an equal volume of chloroform. RNA samples were ethanol precipitated and resuspended in water. Total RNA was quantified by OD_{260} readings. RNA samples were treated with DNase (Invitrogen) according to manufacturer's instructions. cDNA was synthesized using gene-specific primers (see **Supplementary Table 3** online) and Superscript III reverse transcriptase (Invitrogen) according to the manufacturer's instructions. qRT-PCR was carried out on this cDNA using an iCycler iQ system (BioRAD). Samples were prepared using the iQ SYBR green supermix and primer pairs specific for different templates (see **Supplementary Table 3** online) on dilution series of the cDNA, according to the manufacturer's instructions. Data were analyzed using the iCycler iQ software.

***In vitro* antiswitch affinity experiments.** Antiswitch and target sequences were PCR amplified with primers containing a T7 polymerase promoter. RNA was transcribed using Ampliscribe T7 transcription kits (Epicentre) according to manufacturer's instructions, except that transcription was carried out at 42 °C and for gel-shift assays antiswitches were radiolabeled by the addition of [α-^{32}P]-UTP to the transcription mix. The RNA was purified on a 15% denaturing gel, eluted, ethanol precipitated and resuspended in water. RNA was quantified by OD_{260} readings. For nuclease mapping, antiswitches were 5′ end labeled with fluorescein (Molecular Probes) by incubating 25 μg of RNA with a phosphate-reactive label, dissolved in DMSO (Sigma), in labeling buffer (0.12 M methylimidazole pH 9.0, 0.16 M EDAC) for 4 h, according to the manufacturer's instructions. Labeled RNA was purified by ethanol precipitation and run on a 12% denaturing gel. Fluorescent bands were excised from the gel, eluted into water for 3 h at 37 °C and ethanol precipitated.

For gel shift assays, equimolar amounts (5 nM) of radiolabeled antiswitches and target RNA were incubated in varying concentrations of theophylline at 23 °C for 30 min in 15 μl buffer (50 mM Tris-HCl, pH 8.0, 100 mM NaCl, 5 mM $MgCl_2$). After the incubation, 10% glycerol was added to the RNA-target-ligand mixtures and RNA complexes were separated from free RNA by electrophoresis at 125 V on an 8% polyacrylamide gel in 1× Tris-borate buffer at 23 °C for several hours. Gels were dried and antiswitch mobility was imaged on a FX phosphorimager (BioRAD).

For nuclease mapping, fluorescein-labeled antiswitch RNA was resuspended in buffer (50 mM Tris-HCl, pH 8.0, 100 mM NaCl, 5 mM $MgCl_2$), denatured

at 65 °C for 3 min, and allowed to slow cool to 23 °C, antiswitch RNA was incubated with varying concentrations of theophylline at 23 °C for 15 min. RNase T1 (Ambion) was added to the antiswitch-ligand mixture and incubated at 23 °C for 15 min. Cleavage products were visualized using laser-induced fluorescence capillary electrophoresis on a P/ACE MDQ machine (Beckman) using a single-stranded nucleic acid analysis kit (Beckman) according to manufacturer's instructions.

RNA free energy calculations. RNA free energy was calculated with RNAstructure version 3.71 (ref. 32).

Note: Supplementary information is available on the Nature Biotechnology website.

ACKNOWLEDGMENTS

We thank S.V. Avery, A. Miyawaki and K. Weis for providing genes and plasmids used in assembling the constructs described in this work. This work was supported by startup funds provided by the California Institute of Technology.

COMPETING INTERESTS STATEMENT

The authors declare competing financial interests (see the *Nature Biotechnology* website for details).

Received 1 October 2004; accepted 5 January 2005
Published online at http://www.nature.com/naturebiotechnology/

1. Banerjee, D. & Slack, F. Control of developmental timing by small temporal RNAs: a paradigm for RNA-mediated regulation of gene expression. *Bioessays* **24**, 119–129 (2002).
2. Kramer, C., Loros, J.J., Dunlap, J.C. & Crosthwaite, S.K. Role for antisense RNA in regulating circadian clock function in *Neurospora crassa*. *Nature* **421**, 948–952 (2003).
3. Ellington, A.D. & Szostak, J.W. *In vitro* selection of RNA molecules that bind specific ligands. *Nature* **346**, 818–822 (1990).
4. Tuerk, C. & Gold, L. Systematic evolution of ligands by exponential enrichment: RNA ligands to bacteriophage T4 DNA polymerase. *Science* **249**, 505–510 (1990).
5. Good, L. Diverse antisense mechanisms and applications. *Cell. Mol. Life Sci.* **60**, 823–824 (2003).
6. Good, L. Translation repression by antisense sequences. *Cell. Mol. Life Sci.* **60**, 854–861 (2003).
7. Vacek, M., Sazani, P. & Kole, R. Antisense-mediated redirection of mRNA splicing. *Cell. Mol. Life Sci.* **60**, 825–833 (2003).
8. Bartel, D.P. MicroRNAs: genomics, biogenesis, mechanism, and function. *Cell* **116**, 281–297 (2004).
9. Scherer, L. & Rossi, J.J. Recent applications of RNAi in mammalian systems. *Curr. Pharm. Biotechnol.* **5**, 355–360 (2004).
10. Lilley, D.M. The origins of RNA catalysis in ribozymes. *Trends Biochem. Sci.* **28**, 495–501 (2003).
11. Mandal, M. & Breaker, R.R. Adenine riboswitches and gene activation by disruption of a transcription terminator. *Nat. Struct. Mol. Biol.* **11**, 29–35 (2004).
12. Winkler, W., Nahvi, A. & Breaker, R.R. Thiamine derivatives bind messenger RNAs directly to regulate bacterial gene expression. *Nature* **419**, 952–956 (2002).
13. Winkler, W.C., Nahvi, A., Roth, A., Collins, J.A. & Breaker, R.R. Control of gene expression by a natural metabolite-responsive ribozyme. *Nature* **428**, 281–286 (2004).
14. Barrick, J.E. *et al.* New RNA motifs suggest an expanded scope for riboswitches in bacterial genetic control. *Proc. Natl. Acad. Sci. USA* **101**, 6421–6426 (2004).
15. Yelin, R. *et al.* Widespread occurrence of antisense transcription in the human genome. *Nat. Biotechnol.* **21**, 379–386 (2003).
16. Lavorgna, G. *et al.* In search of antisense. *Trends Biochem. Sci.* **29**, 88–94 (2004).
17. Hermann, T. & Patel, D.J. Adaptive recognition by nucleic acid aptamers. *Science* **287**, 820–825 (2000).
18. Cox, J.C. *et al.* Automated selection of aptamers against protein targets translated *in vitro*: from gene to aptamer. *Nucleic Acids Res.* **30**, e108 (2002).
19. Jhaveri, S., Rajendran, M. & Ellington, A.D. *In vitro* selection of signaling aptamers. *Nat. Biotechnol.* **18**, 1293–1297 (2000).
20. Roth, A. & Breaker, R.R. Selection *in vitro* of allosteric ribozymes. *Methods Mol. Biol.* **252**, 145–164 (2004).
21. Stojanovic, M.N. & Kolpashchikov, D.M. Modular aptameric sensors. *J. Am. Chem. Soc.* **126**, 9266–9270 (2004).
22. Smolke, C.D., Carrier, T.A. & Keasling, J.D. Coordinated, differential expression of two genes through directed mRNA cleavage and stabilization by secondary structures. *Appl. Environ. Microbiol.* **66**, 5399–5405 (2000).
23. Isaacs, F.J. *et al.* Engineered riboregulators enable post-transcriptional control of gene expression. *Nat. Biotechnol.* **22**, 841–847 (2004).
24. Yen, L. *et al.* Exogenous control of mammalian gene expression through modulation of RNA self-cleavage. *Nature* **431**, 471–476 (2004).
25. Buskirk, A.R., Landrigan, A. & Liu, D.R. Engineering a ligand-dependent RNA transcriptional activator. *Chem. Biol.* **11**, 1157–1163 (2004).
26. Weiss, B., Davidkova, G. & Zhou, L.W. Antisense RNA gene therapy for studying and modulating biological processes. *Cell. Mol. Life Sci.* **55**, 334–358 (1999).
27. Scherer, L.J. & Rossi, J.J. Approaches for the sequence-specific knockdown of mRNA. *Nat. Biotechnol.* **21**, 1457–1465 (2003).
28. Nutiu, R. & Li, Y. Structure-switching signaling aptamers. *J. Am. Chem. Soc.* **125**, 4771–4778 (2003).
29. Zimmermann, G.R., Wick, C.L., Shields, T.P., Jenison, R.D. & Pardi, A. Molecular interactions and metal binding in the theophylline-binding core of an RNA aptamer. *RNA* **6**, 659–667 (2000).
30. Zimmermann, G.R., Jenison, R.D., Wick, C.L., Simorre, J.P. & Pardi, A. Interlocking structural motifs mediate molecular discrimination by a theophylline-binding RNA. *Nat. Struct. Biol.* **4**, 644–649 (1997).
31. Gouda, H., Kuntz, I.D., Case, D.A. & Kollman, P.A. Free energy calculations for theophylline binding to an RNA aptamer: Comparison of MM-PBSA and thermodynamic integration methods. *Biopolymers* **68**, 16–34 (2003).
32. Mathews, D.H. *et al.* Incorporating chemical modification constraints into a dynamic programming algorithm for prediction of RNA secondary structure. *Proc. Natl. Acad. Sci. USA* **101**, 7287–7292 (2004).
33. Taira, K., Nakagawa, K., Nishikawa, S. & Furukawa, K. Construction of a novel RNA-transcript-trimming plasmid which can be used both *in vitro* in place of run-off and (G)-free transcriptions and *in vivo* as multi-sequences transcription vectors. *Nucleic Acids Res.* **19**, 5125–5130 (1991).
34. Samarsky, D.A. *et al.* A small nucleolar RNA: ribozyme hybrid cleaves a nucleolar RNA target *in vivo* with near-perfect efficiency. *Proc. Natl. Acad. Sci. USA* **96**, 6609–6614 (1999).
35. Mateus, C. & Avery, S.V. Destabilized green fluorescent protein for monitoring dynamic changes in yeast gene expression with flow cytometry. *Yeast* **16**, 1313–1323 (2000).
36. Koch, A.L. The metabolism of methylpurines by *Escherichia coli*. I. Tracer studies. *J. Biol. Chem.* **219**, 181–188 (1956).
37. Berens, C., Thain, A. & Schroeder, R. A tetracycline-binding RNA aptamer. *Bioorg. Med. Chem.* **9**, 2549–2556 (2001).
38. Nagai, T. *et al.* A variant of yellow fluorescent protein with fast and efficient maturation for cell-biological applications. *Nat. Biotechnol.* **20**, 87–90 (2002).
39. Watkins, S.M. & German, J.B. Metabolomics and biochemical profiling in drug discovery and development. *Curr. Opin. Mol. Ther.* **4**, 224–228 (2002).
40. Khosla, C. & Keasling, J.D. Metabolic engineering for drug discovery and development. *Nat. Rev. Drug Discov.* **2**, 1019–1025 (2003).
41. Kobayashi, H. *et al.* Programmable cells: interfacing natural and engineered gene networks. *Proc. Natl. Acad. Sci. USA* **101**, 8414–8419 (2004).
42. Sambrook, J. & Russell, D.W. *Molecular cloning: a laboratory manual*, edn. 3 (Cold Spring Harbor Laboratory Press, Cold Spring Harbor, NY, 2001).
43. Sikorski, R.S. & Hieter, P. A system of shuttle vectors and yeast host strains designed for efficient manipulation of DNA in *Saccharomyces cerevisiae*. *Genetics* **122**, 19–27 (1989).
44. Gietz, R. & Woods, R. Transformation of yeast by lithium acetate/single-stranded carrier DNA/polyethylene glycol method. in *Guide to Yeast Genetics and Molecular and Cell Biology*, Part B, vol. 350 (eds. Guthrie, C. & Fink, G.) 87–96 (Academic Press, San Diego, 2002).
45. Caponigro, G., Muhlrad, D. & Parker, R. A small segment of the MAT alpha 1 transcript promotes mRNA decay in *Saccharomyces cerevisiae*: a stimulatory role for rare codons. *Mol. Cell. Biol.* **13**, 5141–5148 (1993).